Critical thickness for interface misfit dislocation formation in two-dimensional materials

Brian C. McGuigan, Pascal Pochet, and Harley T. Johnson

Phys. Rev. B **93**, 214103 — Published 6 June 2016

DOI: 10.1103/PhysRevB.93.214103

Critical thickness for interface misfit dislocation formation in 2D materials

Brian C. McGuigan,[1] Harley T. Johnson,[1,2] and Pascal Pochet[3,2]

[1] *Department of Mechanical Science and Engineering*
University of Illinois at Urbana-Champaign, Urbana, Illinois 61801, United States
[2] *Université Grenoble-Alpes, Grenoble 38000, France*
[3] *Atomistic Simulation Laboratory (L_Sim)*
CEA, INAC F-38054, Grenoble 38000, France

(Dated: May 12, 2016)

In-plane heterostructures of 2D materials form interface misfit dislocations to relieve lattice mismatch strain, much like heterostructures of 3D materials. Here, using graphene-hexagonal boron nitride (h-BN) as a model system, we consider interface misfit dislocations in 2D lateral heterostructures resting on a flat support layer that prevents out-of-plane deformation. Using an accurate empirical interatomic potential, we carry out a rigorous energetic analysis of the graphene/h-BN interface with 5-7 or 8-6 dislocation cores. We define and extract critical thicknesses for the formation of an interface misfit dislocation in the heterostructure, for the limiting cases when the h-BN or graphene domains are significantly different in size (equivalent to the classic 3D thin film critical thickness problem), and the intermediate case, where the h-BN and graphene domains are of comparable size (equivalent to the classic 3D compliant substrate problem). This makes it possible to compare the alternative dislocation core structures and to determine the resulting dislocation core energy in a continuum analysis. It also reveals a design space where defect-free heterostructures can be grown.

Keywords: Graphene, hexagonal boron nitride, critical thickness, misfit dislocation, interface, heteroepitaxy

I. INTRODUCTION

Two-dimensional (2D) materials such as graphene have the potential to revolutionize nanoelectronics,[1] just as silicon and other bulk (3D) semiconductor materials did in microelectronics in recent decades. As in the case of 3D materials, the promise of graphene and other 2D materials rests on the possibility of designing heterostructures[2,3] in which opto-electronic properties can be engineered through control of energy band alignment,[4] built-in fields, carrier mobilities, *etc.* One class of 2D materials heterostructures are referred to as vertically aligned heterostructures and rely on van der Waals stacking, for which the relative misorientation of the sheet is found to be the key parameter. A second class of 2D material heterostructures relies on lateral interfaces and has been successfully grown in both the honeycomb (i.e. hexagonal)[5] and in the transition metal dichalcogenide (TMDC)[6] families; this configuration consists of a 2D-film and a 2D-substrate, resting on a support layer, as shown in Fig. 1(a). Rapid progress has been made recently in fabricating and characterizing this class of heterostructures, also known as parallel-stitched materials.[7] As in 3D materials, the success of such heterostructures requires engineering the strain and associated interfacial defects, which can otherwise create significant problems for resulting device properties.

The objective of the present work is to use an atomistic framework to understand interface misfit dislocations in 2D materials, unifying the understanding of core structure and the role of the defects in relieving lattice mismatch strain in 2D lateral heterostructures. In order to compare to the 3D case, we describe such in-plane heterostructures as consisting of a 2D-film and a 2D-substrate, as shown in Fig. 1(a). The 2D-substrate would describe the first deposited material on a supporting metallic layer, while the 2D-film would be the second deposited material, which would be expected to grow from the island edge of the 2D-substrate. For the sake of simplicity the 2D-film and the 2D-substrate are described hereafter as the *film* and the *substrate* and the supporting metallic layer is referred to as the *support*.

We choose the graphene/h-BN system as a prototype for such lateral heterostructures as it is simpler than TMDC systems and has been grown on different supports[8–10] since the pioneering work of Ci *et al.*[5] Indeed different supports will give rise to varying strain conditions due to the degree of coherency between the heterostructure and the support;[11] thus the interfacial strain relief will also change. Finally, to the best of our knowledge, 2D misfit dislocations have only been reported in the graphene/h-BN[10] system while they are absent by definition in TMDC heterostuctures based on the same chalcogenides[2,6] and not observed in mixed chalcogenide WSe_2-MoS_2 junctions[12,13].

II. RESULTS AND DISCUSSION

A. Superlattice configuration

We study the graphene/h-BN interface in several separate cases using a superlattice structure shown in Fig. 1(b) and 1(c). With this configuration it is possible to avoid edge reconstruction, image forces, and stoichiometry issues arising due to the presence of free surfaces[10]. Instead, it assumes periodicity in the growth direction (y in Fig. 1(b)) resulting in two nonequivalent graphene/h-

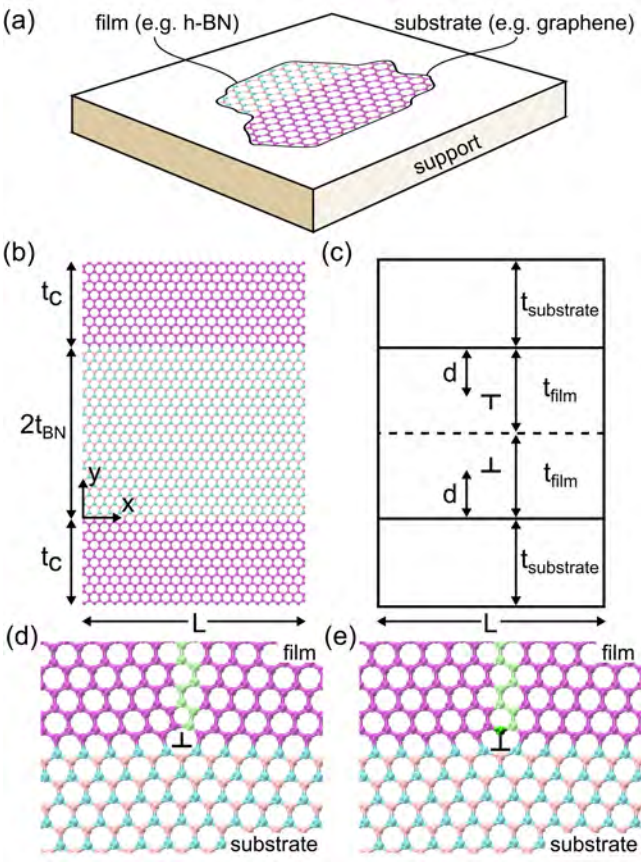

FIG. 1. (a) schematic of the 2D film, 2D substrate, and support. (b) Coherent heterostructure supercell with length L, h-BN film thickness t_{BN}, and graphene substrate thickness t_C. (c) Schematic of the superlattice geometry, with dislocations each offset from the interface by d. By symmetry, this geometry is equivalent to the case of a thin film (with a free surface) growing on a substrate, with film thickness t_{film} and substrate thickness $t_{substrate}$. (d),(e) Core reconstructions for the case of a graphene film on an h-BN substrate with 5-7 and 8-6 cores. The carbon atoms shown in green represent the extra plane used to construct the dislocation. The dark green atom is inserted into the 5-7 core to create the 8-6 core.

BN interfaces. By symmetry, this configuration is mechanically equivalent to a film with a free surface growing on a substrate (where the symmetry plane equivalent to the free surface is shown with the dotted line in Fig. 1(c)). The interfacial direction (x) is also periodic with an interfacial length L≈105 Å, or 42 unit cells, which is equal to the expected average misfit dislocation spacing along a fully relaxed graphene/h-BN heterointerface. The choice of this unit cell size is justified by arguing that full strain relief can be achieved by formation of one interface misfit dislocation in the periodic unit cell. The system is constrained against out-of-plane bending, as it would be if it were in uniform contact with the growth support. The supercells considered here remain rectangular and are analyzed at varying film/substrate thicknesses in the y direction. The dislocation cores are also assumed to manifest in the film material. Classical potentials fitted[14] to the C-C, B-N, C-B, and C-N bond lengths are used to describe the energy of the atomistic supercell domain. In order to compare energies of configurations with and without dislocations, we define a defect formation energy that accounts for the actual number of C-C or B-N atom pairs in the supercell. The details of the defect formation energy analysis are presented in Appendix A.

Due to its smaller lattice parameter, when the graphene film is forced to accommodate the strain associated with an epitaxial relationship to an h-BN substrate, it does so through the formation of an interface dislocation with the characteristic 5-7 core[10,15] structure as shown in Fig. 1(d). This structure can be realized by first forcing a fully strained graphene layer into registry with the h-BN substrate and then allowing relaxation through the insertion of an armchair column of carbon atoms perpendicular to the interface as depicted by the light green atoms. In the zig-zag interface orientation considered here, this is equivalent to the insertion of a zigzag chain of carbon atoms at 60 degrees or 120 degrees relative to the interface. The difference between the 5-7 core structure and a 8-6 core structure[15], illustrated in Fig. 1(d) and 1(e), is the removal or insertion of a single carbon atom at the core, shown in dark green in 1(e). This is equivalent to a vacancy or interstitial mediated dislocation climb mechanism. Conversely, when the h-BN film is forced to accommodate the strain associated with an epitaxial relationship to a graphene substrate, it also does so through formation of an interface dislocation with equivalent cores, the details of which are presented in Appendix B.

In the following, these film/substrate and core combinations are first analyzed in the limit that the substrate is much larger than the film thickness, with varying embedded core distance, d, as shown in Fig. 1(c). The film is assumed to fully accommodate the misfit strain by adopting the stress-free lattice parameter of the substrate. We model a substrate layer of finite-thickness to represent the infinite substrate and to capture the elastic behavior near the interface, but this case can be understood to mimic film growth on an infinitely thick substrate. After considering the two limiting cases of thin film on thick substrate, we consider the more general case in which the superlattice takes a lattice parameter between that of h-BN and graphene. This case can be understood to mimic a more realistic case where the mismatch strain is shared by the h-BN and the graphene – the so-called compliant substrate case. The total supercell thickness and interfacial length is allowed to vary during minimization and is dictated by the film/substrate thickness ratio. The core is positioned at the interface with an embedded core distance d=0 Å.

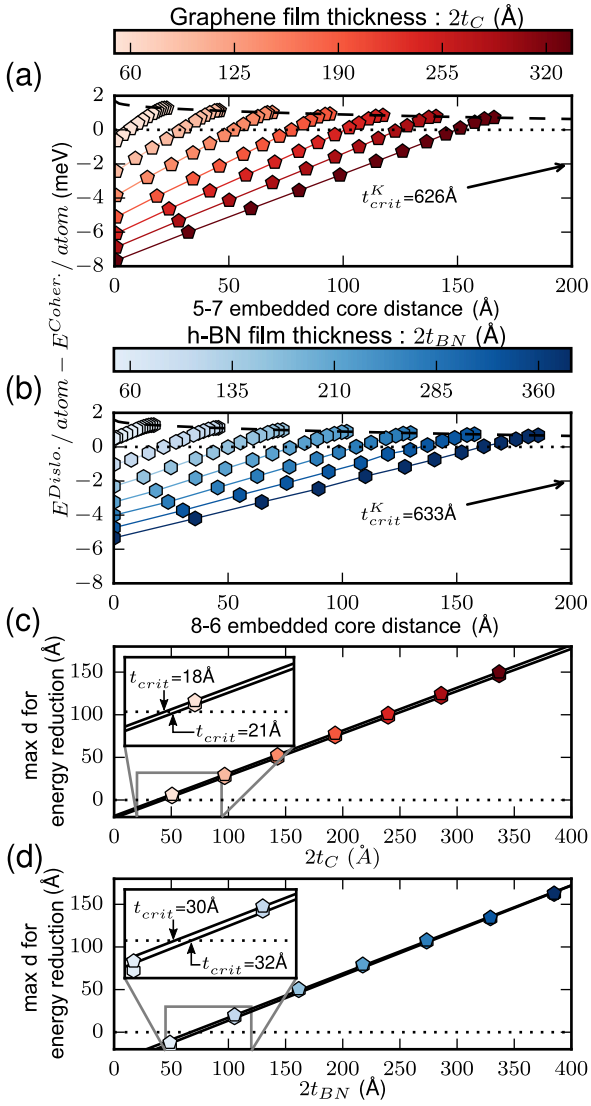

FIG. 2. (a): Embedded dislocation stability analysis of a C film on a thick BN layer for the 5-7 dislocation core. $(E^{Dislo.}/atom)-(E^{Coher.}/atom) < 0$ represents the condition for which dislocation formation is energetically favorable. (b): Embedded dislocation stability analysis of an h-BN film on a thick C layer for the 8-6 dislocation core. The other possible core and film/substrate combinations are also considered.[15] The dashed lines in (a) and (b) bound the upper limit for the embedded core distance. An upper bound to the kinetic critical thickness is found by extrapolating to the zero crossings of these lines and is noted for each case in the figure. (c),(d): Maximum embedded core distance for energy reduction, (c) for a C film on a thick h-BN layer and (d) for a h-BN film on a thick C layer. The thermodynamic critical thickness for a C film on a thick h-BN substrate is interpolated as 41.7 Å for the 8-6 core and 35.0 Å for the 5-7 core. The thermodynamic critical thickness for the h-BN film on thick C is interpolated as 63.4 Å for the 8-6 core and 60.7 Å for the 5-7 core.

B. Strain relaxation as a function of dislocation core position

The results of the embedded dislocation core stability analysis are shown in Fig. 2. In Fig.2(a), we consider a 5-7 dislocation core, embedded at depth d in a graphene film on a much thicker h-BN substrate. In Fig.2(b), we consider the 8-6 dislocation core in h-BN on a much thicker graphene substrate. The other core and film/substrate considerations are approached similarly and presented in Appendix C.

In the cases shown in Fig. 2, misfit strain is partially accommodated in the y direction during minimization, while the unit cell size parallel to the interface is fixed according to substrate lattice parameter. The configuration is considered to be energetically favorable when the formation energy with the dislocation becomes less than the formation energy of an equivalent sized coherent supercell, *i.e.* for negative values of the dependent variable. The zero crossings for these curves are summarized for the different film thicknesses and core reconstructions in Fig. 2 (c and d) which show the maximum embedded core distance at which the dislocation can still provide energy reduction. The film thickness (actually the double thickness $2t_C$ or $2t_{BN}$ in the supercell configuration) at which this maximum embedding distance is zero is the critical thickness. This critical thickness corresponds to the thermodynamic condition at which the energetic cost of the dislocation is balanced by the strain relief it provides to the system; this is equivalent to the well known Matthews-Blakeslee critical thickness in 3D film growth.[16] In each film/substrate case, the 5-7 core is slightly favored over the 8-6 core. For a graphene film on an infinite h-BN substrate, the 5-7 and 8-6 cores have a t_{crit} of 18 Å and 21 Å respectively. An h-BN film grown on an infinite graphene substrate has a larger t_{crit} of 30 Å and 32 Å for the 5-7 and 8-6 cores respectively.

A second, alternative critical thickness can be deduced from this analysis, and can be considered as an upper bound to a kinetic limit, t^K_{crit}. This limit is observed when, at the limit that the embedded core distance reaches $d{\approx}t_{film}$, the system is still able to reduce its energy relative to the coherent case, *i.e.* it is the film thickness above which it is always energetically favorable to accommodate the insertion of a dislocation at the free surface. In 3D thin film mechanics this limit corresponds to the critical thickness for homogeneous nucleation of a misfit dislocation half-loop at a free surface. This limit is found by extrapolating, from the largest embedded core distances for a given film thickness to the zero crossing, or the case for which all points in the curve are below zero. The curves associated with this extrapolation are denoted by the dashed lines in Fig. 2(a-b). The t^K_{crit} values from these dashed line zero crossings are also shown. For a graphene film on an infinite h-BN substrate, the formation of an 8-6 core (t^K_{crit} = 620 Å) is marginally favored over the 5-7 core (t^K_{crit} = 626 Å) in the kinetic growth limit. However, for a h-BN film on graphene, the

formation of a 5-7 core (t^K_{crit} = 551 Å) is significantly favored over the 8-6 core (t^K_{crit} = 633 Å). These values are much larger than the thermodynamic critical thickness, but are less realistic, because they correspond to the extreme case of perfect homogeneous dislocation nucleation at a free surface and to the case in which dislocation cores are immobile after the growth process – while the 8-6 core has been predicted to be mobile relative to its 5-7 counterpart.[17]

The critical thickness values computed so far all depend on the assumption that the *film* thickness is much smaller than the *substrate* thickness, but in some recent experimental work on h-BN/graphene interfaces, the system is better described by interfaces between h-BN and graphene domains of comparable dimension. While precise dislocation core structures have yet to be determined experimentally, moiré patterns reported in recent experiments[10] are compatible with either 5-7 or 8-6 core structures. Furthermore, in these experiments there is some evidence that dislocations may exist in configurations at some small distance from the interface, and that there may be elastic interactions with corners and facets along the interface.

C. Strain-balanced (compliant substrate) case

These observations, along with the possibility of partial coherency between the film/substrate system and the support layer, suggest that it is necessary to understand the critical thickness condition for the intermediate strain-balanced case, where neither the film nor the substrate is in a strain-free condition. In the intermediate case, instead of h-BN fully accommodating the strain associated with epitaxy on the graphene substrate, or graphene fully accommodating the strain associated with the h-BN substrate, one can expect that the system will relax to an intermediate lattice parameter between that of h-BN and graphene.

This intermediate case can be shown to correspond to the classic 3D compliant substrate critical thickness problem.[18] The critical thickness in the present case is determined by balancing the work done by the full unrelaxed mismatch strain W_m, the energetic cost of the dislocation due to the work required to overcome the image forces W_y^{Image} and W_x^{Image}, and the energy of the dislocation E_{core} inside the cutoff radius r_0, according to $W_m + 2W_y^{Image} + 2W_x^{Image} + 2E_{core} = 0$. The work done by the image forces is proportional to $\ln(\alpha/r_0)$ where α is a function of the thickness ratio of the film and substrate. (Additional details are provided in Appendix C.) Thus, both E_{core} and r_0 can be considered as fitting parameters in the continuum critical thickness theory. The same atomistic supercell configuration, shown in Fig. 1, is used to compute the atomistic total energy for comparison to the compliant substrate continuum critical thickness criterion, by varying the film/substrate thickness ratio; this calculation can then be used to *determine* values for E_{core} and r_0. The supercell boundaries remain periodic and rectangular, but the box size is allowed to vary during minimization in both the interface (x) and growth (y) directions. This allows the system to share the mismatch strain between both the film and substrate. The same criterion is used to distinguish energetically favorable configurations for dislocation formation over a range of film/substrate thickness values as detailed in Appendix C.

A full comparison between the calculated and theoretical critical thickness criteria is then shown in Fig. 3. The elastic moduli used in the continuum analysis are determined from the interatomic potentials. The critical thickness from the continuum theory is shown as a dashed or dotted line while the critical thickness computed atomistically is shown with the symbols. The primary horizontal axis is the log of the film/substrate thickness ratio. For a particular film/substrate thickness ratio, defect-free h-BN growth on a much thicker graphene substrate can occur up to the condition plotted in blue; defect-free graphene growth on a much thicker h-BN substrate can occur up to the condition plotted in red. The distribution of mismatch strain is represented using the two additional horizontal axes. The central region along the x-axis, where the strain is balanced between the film and substrate, represents an interesting design space for defect-free heterostructure growth, while the limiting cases of film growth on substrates of infinite thickness (the so-called Matthews-Blakeslee condition[16]) are shown at the extreme values on the thickness ratio axis. Fig. 3(a) shows that the continuum and atomistic critical thickness values are in reasonable agreement even when the free parameters E_{core} and r_0 are chosen to be 0 eV and $|b|$ (as shown by the solid lines), respectively, as is typically the case in 3-D critical thickness theory.

Whether the dislocation is in graphene or in h-BN, the 5-7 core (shown with the five-sided symbols) costs the system less energy to accommodate than the 8-6 core (shown with the six-sided symbols), and thus leads to a lower observed critical thickness. This trend is more pronounced in the graphene film (as shown in red). When the dislocation is in a h-BN film on a graphene substrate, however, the energetic cost of the homopolar bond in the 5-7 case raises the energy that the system must pay to accommodate the dislocation, almost to a level equivalent to that of an 8-6 core (as shown in blue). Thus, the preference that graphene shows for the 5-7 core over the 8-6 core, which corresponds to a critical thickness difference of roughly 8Å, nearly vanishes in h-BN, due to the effect of stoichiometry at the core. This is consistent with experimental observations of *heart-shape* moiré defects near and at the graphene/h-BN interface[10].

The agreement between the continuum model and the atomistic model is greatly improved by using a non-linear least squares curve fit to find values for r_0 and E_{core}. In the first case, as shown in Fig. 3(a), the fitting procedure is used to find r_0, while leaving $E_{core} = 0$. In the second case, as shown in Fig. 3(b), values are found for

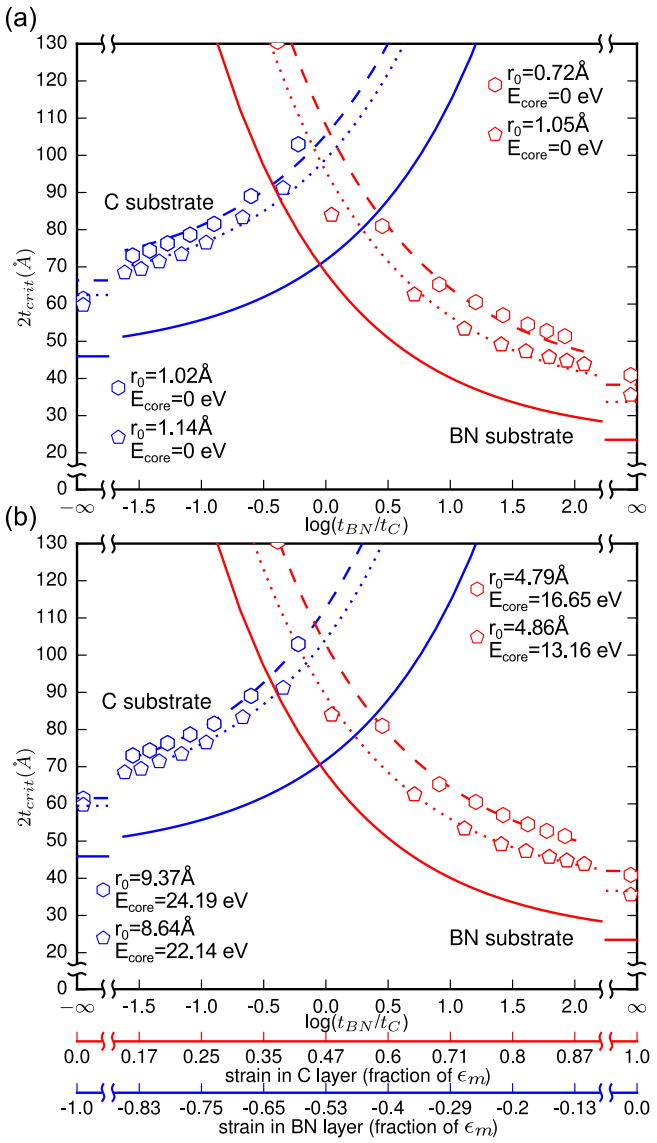

FIG. 3. Critical thickness of h-BN/graphene system, as a function of the ratio of layer thicknesses (primary horizontal axis) and as a function of the misfit strain in the C and h-BN layers (secondary horizontal axes). At the left and right extremes on the horizontal axis, the system consists of a thin layer on an infinitely thick substrate; at the center, the system is approximately strain-balanced. The atomistic results are plotted against the continuum theoretical results with (a) cutoff radius r_0 fitted via a nonlinear least squares method, and $E_{core} = 0$, and (b) both r_0 and E_{core} fitted using a nonlinear linear squares method. The case with cutoff radius $r_0 = |b|$ and $E_{core} = 0$, used in traditional 3D critical thickness theory, is depicted by the solid lines. Five-sided symbols refer to the 5-7 core with dotted theoretical curves; six-sided symbols refer to the 8-6 core with dashed theoretical curves. The corresponding fitted values for the cutoff radius and core energy are shown in the inset.

both r_0 and E_{core}. This process results in an even better fit between the continuum and atomistic critical thicknesses. The determined fitting parameters are summarized in Fig. 3(a),(b). Without fitting for a nonzero core energy, the best-fit cutoff radius is found to be smaller than b, (or r_0 =0.2b-0.46b), and the error norm of the fit is larger than the cutoff radius itself. With a non-zero core energy (of 13-25 eV), the overall fit is better, and the best-fit cutoff radius is significantly larger (r_0 =1.92b-3.76b); in this case the error norm is significantly smaller than the fitted cutoff radius. Not surprisingly, there are significant differences between the h-BN and graphene cases, and between the 5-7 and 8-6 cores, illustrating the importance of considering the detailed structure and energetics of the dislocation cores in these 2D material lateral heterostructures.

III. SUMMARY AND CONCLUSIONS

In summary, we have examined the stability of graphene/h-BN lateral heterostructures against formation of interface misfit dislocations. We identify the classic thermodynamic critical thickness as the smallest 2D-film thickness for which it is energetically favorable to insert a full dislocation on the film side of the interface – *i.e.* the condition at which the energy gained by strain relief balances the energetic cost of inserting the dislocation, including both the elastic self-energy and the core energy. It is found that the graphene critical thickness is 18 Å for the 5-7 core and 21 Å for the 8-6 core, while the h-BN critical thickness is 30 Å for the 5-7 core and 32 Å for 8-6 core. Thus, the 8-6 core is energetically more costly for both materials, but the difference between the 5-7 and 8-6 core energies is less for h-BN than for graphene, as one would expect due to the energetic penalty associated with homopolar bonding in h-BN. This trend is also observed in the strain-balanced or compliant substrate critical thickness analysis, where the the system is allowed to relax to a lattice parameter between that of bulk h-BN and bulk graphene. It is shown that when the 2D-film and 2D-substrate are of nearly equal thickness, the critical thickness is 50-100% greater than in the thick substrate limiting cases. The atomistic critical thickness results fit the plane stress continuum compliant substrate critical thickness results very accurately with dislocation core cutoff radii of 8-9 Å and core energies of 22-24 eV depending on whether the core is of 5-7 or 8-6 type. The analysis has significant implications for the design of defect free lateral heterostructures of h-BN and graphene, and may be extended to other 2D materials like TMDC.

ACKNOWLEDGMENTS

H.T.J. acknowledges support from a Fulbright Fellowship and from Université Joseph Fourier, Grenoble, through an invited professorship. B.C.M. acknowledges the support of the National Science Foundation Graduate Research Fellowship Program under Grant Number

DGE-1144245 and a NSF GROW (Graduate Research Opportunities Worldwide) Award.

Appendix A: Computing the formation energy

Classical interatomic potentials can be used to accurately describe structural properties in h-BN/graphene systems. Potentials such as Tersoff-Brenner[19–21], REBO[22], AIREBO[23] and LCBOPII[24], are fit according to a combination of theoretically predicted or experimentally observed criteria such as lattice constants/elastic moduli[25], interatomic bond lengths[26], cohesive/defect energies[27], and phonon dispersions[28,29]. However, in most cases the potentials are parameterized for BN or graphene alone while a reliable description of the intermixing among B-N-C species is unavailable. In some cases BN is represented by a generic atom that imitates the expected elastic behavior, in which case the BN is treated as a monolithic material, without distinguishing the separate B and N species.[30] In the present study a Tersoff potential is used,[14] which relies on a fitting procedure for a more accurate description of B-C and N-C bonding based on *ab initio* energetics, which is important for an accurate description of the interface.

However, using LAMMPS[31] and this parameterization,[14] the equilibrium lattice constants for h-BN and graphene are found to be 2.498 Å and 2.492 Å respectively. This underestimates the lattice constant difference observed experimentally[32] by 2% absolute. To more closely model the experimental mismatch strain, Tersoff parameters that contain units of length or inverse length are scaled proportionally with their length dependence by the ratio of the parameterized and experimentally observed lattice parameters. This procedure preserves the energetics of the system and modifies only length-scales such that the new lattice constants for h-BN and graphene are 2.52 Å and 2.46 Å respectively.

To compare the relative energies between systems with and without dislocations, an energy of formation approach is used. The energy of formation, E, is defined as

$$E = E_{tot} - (N_{CC}E_{CC} + N_{BN}E_{BN}) \qquad \text{(A1)}$$

where $N_{CC|BN}$ is the number of C-C or B-N atom pairs in the supercell, $E_{CC|BN}$ is the reference energy per C-C or B-N pair in the bulk (unstrained) material, and E_{tot} is the total potential energy of the superlattice given by the Tersoff potential.

Appendix B: Dislocation core structure in h-BN film

As an alternative to the dislocation core structures residing in the graphene film as shown in Fig. 1, we also consider the possibility that the core reconstructs the h-BN film in either the 8-6 configuration or the 5-7 structure, as shown in Fig. 4. The two possible core reconstructions are related by a dislocation climb process, as shown in Fig. 4(a). First, a fully strained h-BN layer is forced into registry with the graphene substrate and then allowed to relax through removal of four BN units perpendicular to the interface; this structure is equivalent to a pair of 8-6 dislocation cores of opposing sign. In order to minimize the total energy in the system, these dislocations move apart, via climb, and approach the upper and lower interfaces. With each atom removed (or vacancy created), the core structure alternates between an 8-6 and a 5-7 reconstruction, until the cores eventually reach the interface, as shown in the final two configurations of Fig. 4(a). The core reconstructions of these two defects show in 4(d) and 4(e) differ by the removal of two atoms near the core resulting in a small climb displacement. The overall stoichiometry is preserved by having each film/substrate interface terminated by a complementary boron/nitrogen-carbon pair, which is necessary for the energy of formation analysis. Locally, however, when the h-BN film forms the 5-7 core reconstruction, it is forced to accommodate a homopolar bond to close the 7-atom ring along the interface (respectively B-B and N-N on each of the two interfaces).

When the film/substrate system is on a crystalline metal support layer, such as Ru(0001), a Moiré pattern is often observed experimentally. Simulated Moiré patterns for the final configurations in Fig. 4(a) are shown in Fig. 4(b) and (c). The patterns are obtained through a low-pass filtered convolution of the film/substrate and support atoms as represented by Gaussian distributions. The resulting patterns for each type of core near the interface show the characteristic "heart-shaped" pattern often observed experimentally.[10] The similarity of these patterns for the 8-6 and 5-7 cores illustrates the difficulty in experimentally identifying the precise dislocation core structure in such systems.

Appendix C: Strain-balanced (compliant substrate) case

It can be readily shown that when the 2D-film and 2D-substrate domains are of comparable thickness, the problem is a variation of the so-called compliant substrate case,[18] in an ideal plane stress configuration, and where equilibrium requires that the in-plane extensional stress in the two layers is equal and opposite, so that

$$M_f t_f \epsilon_f = M_s t_s \epsilon_s, \qquad \text{(C1)}$$

where M is bulk modulus, t is layer thickness, and ϵ is strain. Thus, assuming the two layers have equal bulk modulus, a strain balanced condition can be achieved if $t_{BN} = t_C$. In this case the possible formation of a strain relieving interface misfit dislocation will depend on the

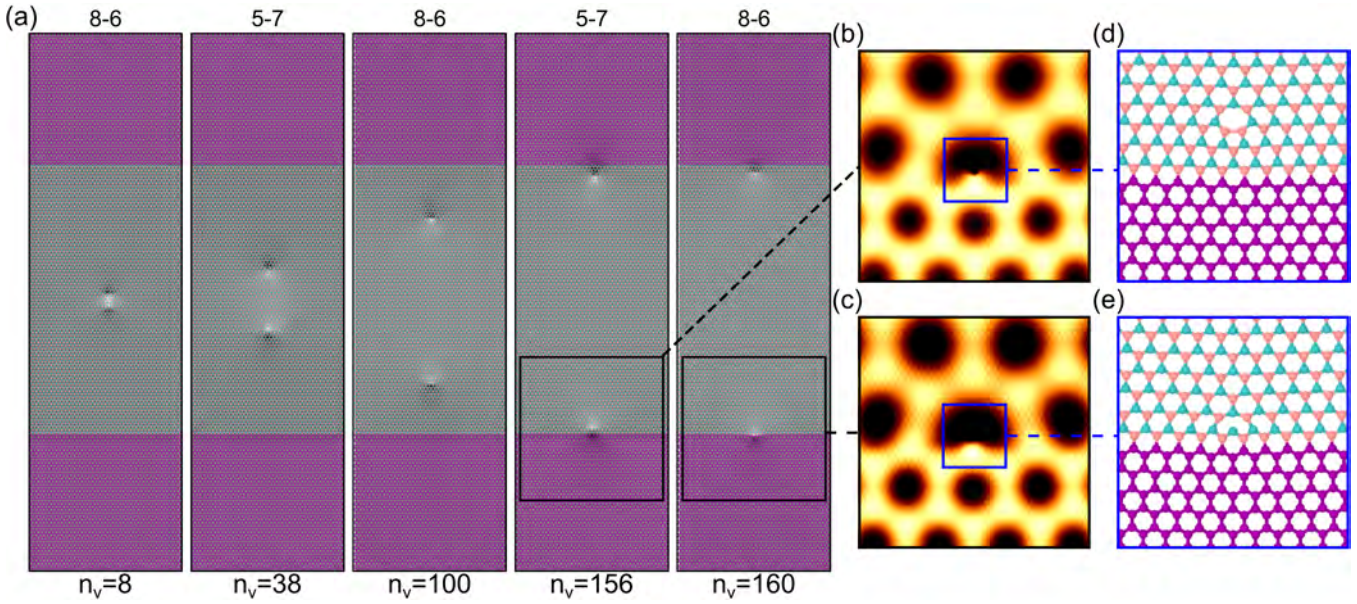

FIG. 4. (a), Schematic showing several intermediate steps in the dislocation climb process through which dislocation cores move to the interfaces to maximize strain relief. The inner material in (a) is h-BN, and the outer material is graphene. The background gray-scale contours represent the minimum negative (light) and maximum positive (dark) hydrostatic virial stress components for each system. The value of n_v denotes the number of vacancies added (atoms removed) in order for the dislocations to climb to their respective positions. (b),(c) Simulated Moiré reconstructions of the final two systems on a Ru(0001) support. (d),(e) Core reconstructions near the interface for a h-BN film on a graphene substrate with 5-7 and 8-6 cores.

layer thickness (or the period of the superlattice), leading to the notion of a critical thickness, as described below.

Strain compatibility between the layers is enforced, or $\epsilon_f - \epsilon_m = \epsilon_s$, and with Eq. (2),

$$\epsilon_f = \epsilon_m \frac{t_s M_s}{t_s M_s + t_f M_f}, \tag{C2}$$

and

$$\epsilon_s = -\epsilon_m \frac{t_f M_f}{t_s M_s + t_f M_f}, \tag{C3}$$

where ϵ_m is the lattice mismatch strain. The amount of energy that may be fully relaxed by the dislocation or, equivalently, the work associated with the full coherent strain field, is given by

$$W_m = 2 M_s \epsilon_s t_s b, \tag{C4}$$

where b is the Burgers vector magnitude of the film material with sign chosen such that $\epsilon_m b > 0$. The cost associated with introducing the dislocation into a periodic supercell with variable length (L) and height ($2t_s + 2t_f$) is then weighed against this possible strain relaxation. The forces on one dislocation from its two half-space image forces in the growth direction are given as

$$F(y)^{Image} = \frac{\mu b^2 (1+\nu)}{4\pi} \left[\frac{1}{2t_s + 2t_f - y} - \frac{1}{y} \right], \tag{C5}$$

where y is the distance from the bottom of the film. The elastic constants μ and ν are chosen based on a weighted linear combination of film and substrate properties, such that μ for example would be $\mu = \mu_f(t_f/(t_s + t_f)) + \mu_s(t_s/(t_s + t_f))$.

The dislocation also experiences image interactions in the interfacial direction, given by

$$F(x)^{Image} = \frac{\mu b^2 (1+\nu)}{4\pi} \left[\frac{1}{L - x} - \frac{1}{x} \right], \tag{C6}$$

where x is the distance from the edge of the system. The self-energy of the dislocation at the interface is the work done in overcoming these image forces as the dislocation is moved to the interface at the center of the unit cell such that

$$\begin{aligned} W_x^{Image} &= -\int_{r_0}^{L/2} F(x)^{Image} dx \\ &= \frac{\mu b^2 (1+\nu)}{4\pi} \ln\left(\frac{L}{4r_0}\right), \end{aligned} \tag{C7}$$

and

$$\begin{aligned} W_y^{Image} &= -\int_{r_0}^{2t_f} F(y)^{Image} dy \\ &= \frac{\mu b^2 (1+\nu)}{4\pi} \ln\left(\frac{2t_s t_f}{r_0(t_s + t_f)}\right), \end{aligned} \tag{C8}$$

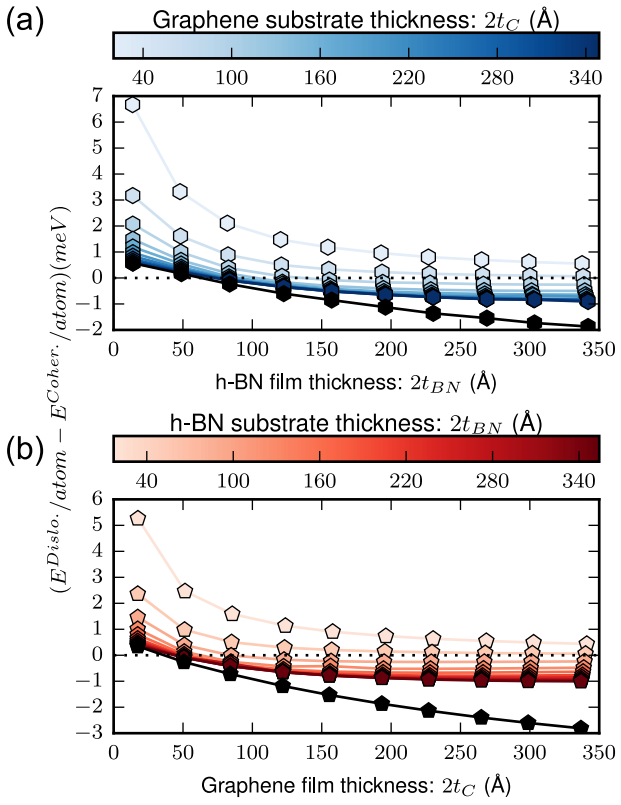

FIG. 5. Compliant substrate analysis for varying t_C, t_{BN} combinations with core at interface (d=0 Å). Film/substrate combinations with $E^{Dislo.}/atom - E^{Coher.}/atom < 0$ represent cases where dislocation formation is energetically favorable. (a) h-BN film on graphene substrate (8-6 core). (b) Graphene film on h-BN substrate. (7-5 core) Results for the h-BN film on graphene substrate (7-5 core) and graphene film on h-BN substrate (8-6 core) are not shown here.

where r_0 is the dislocation core cutoff radius inside which the linear elastic theory breaks down. The condition of zero net work gives the film thickness at which the dislocation cost is overcome by elastic relaxation for a fixed substrate thickness, such that

$$W_m + 2W_y^{Image} + 2W_x^{Image} + 2E_{core} = 0, \qquad \text{(C9)}$$

where E_{core} is the dislocation core energy contained within r_0. In continuum theory for 3D film-substrate systems, this core energy is typically neglected. Here, calculating the system energy atomistically, we are able to find an estimate for this contribution to the energy balance. The same atomistic supercell shown in Fig. 1 is used to compute the formation energy of the interface misfit dislocation in the compliant substrate case. In this case the lateral dimension of the unit cell is allowed to vary so that the misfit strain can be shared by the film and substrate layers, according to the modulus-weighted ratios of their thicknesses, as given in equations C2 and C3.

The results of this calculation are shown in Fig. 5. In Fig. 5(a), the graphene layer is the nominal substrate, so the dislocation is inserted at the interface on the h-BN side. Fig. 5(b) shows the case in which h-BN is the substrate material, and the dislocation is inserted at the interface on the graphene side. All combinations of layer double-thickness from approximately 10 Å to 350 Å are considered, for the 8-6 core in h-BN and the 5-7 core in graphene. Negative values of the energy per atom difference represent cases in which dislocation formation is energetically favorable; *i.e.* the zero-crossings form the critical thickness condition.

[1] B. Dubertret, T. Heine, and M. Terrones, Acc. Chem. Res **48**, 1 (2015).
[2] M.-Y. Li, C.-H. Chen, Y. Shi, and L.-J. Li, Mater. Today **0**, (2015).
[3] T. Niu and A. Li, Progress in Surface Science **90**, 21 (2015).
[4] A. Ramasubramaniam, D. Naveh, and E. Towe, Nano Lett. **11**, 1070 (2011).
[5] L. Ci, L. Song, C. Jin, D. Jariwala, D. Wu, Y. Li, A. Srivastava, Z. F. Wang, K. Storr, L. Balicas, F. Liu, and P. M. Ajayan, Nat. Mater **9**, 430 (2010).
[6] C. Huang, S. Wu, A. M. Sanchez, J. J. P. Peters, R. Beanland, J. S. Ross, P. Rivera, W. Yao, D. H. Cobden, and X. Xu, Nat. Mater **13**, 1096 (2014).
[7] X. Ling, Y. Lin, Q. Ma, Z. Wang, Y. Song, L. Yu, S. Huang, W. Fang, X. Zhang, A. L. Hsu, Y. Bie, Y.-H. Lee, Y. Zhu, L. Wu, J. Li, P. Jarillo-Herrero, M. Dresselhaus, T. Palacios, and J. Kong, Adv. Mater. , (to be published).
[8] Y. Gao, Y. Zhang, P. Chen, Y. Li, M. Liu, T. Gao, D. Ma, Y. Chen, Z. Cheng, X. Qiu, W. Duan, and Z. Liu, Nano Lett. **13**, 3439 (2013).
[9] L. Liu, J. Park, D. a. Siegel, K. F. McCarty, K. W. Clark, W. Deng, L. Basile, J. C. Idrobo, A.-P. Li, and G. Gu, Science **343**, 163 (2014).
[10] J. Lu, L. C. Gomes, R. W. Nunes, a. H. Castro Neto, and K. P. Loh, Nano Lett. **14**, 5133 (2014).
[11] M. S. Bronsgeest, N. Bendiab, S. Mathur, A. Kimouche, H. T. Johnson, J. Coraux, and P. Pochet, Nano Lett. **15**, 5098 (2015).
[12] X. Duan, C. Wang, J. C. Shaw, R. Cheng, Y. Chen, H. Li, X. Wu, Y. Tang, Q. Zhang, A. Pan, J. Jiang, R. Yu, Y. Huang, and X. Duan, Nat. Nanotechnol. **9**, 1024 (2014).
[13] M.-Y. Li, Y. Shi, C.-C. Cheng, L.-S. Lu, Y.-C. Lin, H.-L. Tang, M.-L. Tsai, C.-W. Chu, K.-H. Wei, J.-H. He, W.-H. Chang, K. Suenaga, and L.-J. Li, Science **349**, 524 (2015).
[14] A. Kinaci, J. B. Haskins, C. Sevik, and T. Çağ ın, Phys. Rev. B **86**, 115410 (2012).
[15] A. Zobelli, C. P. Ewels, A. Gloter, G. Seifert, O. Stephan, S. Csillag, and C. Colliex, Nano Lett. **6**, 1955 (2006).
[16] J. Matthews and A. Blakeslee, J. Cryst. Growth **27**, 118 (1974).
[17] X. Zou, M. Liu, Z. Shi, and B. I. Yakobson, Nano Lett. **15**, 3495 (2015).

[18] L. B. Freund and S. Suresh, in *Thin Film Materials* (Cambridge University Press, 2004) pp. 387–463.
[19] J. Tersoff, Phys. Rev. B **37**, 6991 (1988).
[20] J. Tersoff, Phys. Rev. Lett. **61**, 2879 (1988).
[21] D. Brenner, Phys. Rev. B **42**, 9458 (1990).
[22] D. W. Brenner, O. A. Shenderova, J. A. Harrison, S. J. Stuart, B. Ni, and S. B. Sinnott, J. Phys. Condens. Matter **14**, 783 (2002).
[23] S. Stuart, A. Tutein, and J. Harrison, J. Chem. Phys **112**, 6472 (2000).
[24] L. M. Ghiringhelli, J. H. Los, A. Fasolino, and E. J. Meijer, Phys. Rev. B **72**, 214103 (2005).
[25] K. Matsunaga, C. Fisher, and H. Matsubara, Jpn. J. Appl. Phys. **39**, L48 (2000).
[26] V. Verma, V. K. Jindal, and K. Dharamvir, Nanotechnology **18**, 435711 (2007).
[27] K. Albe and W. Möller, Comput. Mater. Sci. **10**, 111 (1998).
[28] L. Lindsay and D. A. Broido, Phys. Rev. B **81**, 205441 (2010).
[29] C. Sevik, A. Kinaci, J. B. Haskins, and T. Çağ ın, Phys. Rev. B **84**, 085409 (2011).
[30] D. Nandwana and E. Ertekin, Nano Lett. **15**, 1468 (2015).
[31] S. Plimpton, J. Comput. Phys. **117**, 1 (1995).
[32] Z. Liu, L. Ma, G. Shi, W. Zhou, Y. Gong, S. Lei, X. Yang, J. Zhang, J. Yu, K. P. Hackenberg, A. Babakhani, J.-C. Idrobo, R. Vajtai, J. Lou, and P. M. Ajayan, Nat. Nanotechnol. **8**, 119 (2013).